CELL ADHESION & MIGRATION
2018, VOL. 12, NO. 3, 228–235
https://doi.org/10.1080/19336918.2017.1346774

Taylor & Francis
Taylor & Francis Group

RESEARCH PAPER

OPEN ACCESS Check for updates

Skeletal muscle regeneration involves macrophage-myoblast bonding

Laura Cristina Ceafalan[a,b], Tudor Emanuel Fertig[a], Alexandru Cristian Popescu[a,b], Bogdan Ovidiu Popescu[a,c], Mihail Eugen Hinescu[a,b], and Mihaela Gherghiceanu[a,b]

[a]Ultrastructural Pathology Laboratory, Victor Babes National Institute of Pathology, Bucharest, Romania; [b]Department of Cellular & Molecular Biology and Histology, School of Medicine, Carol Davila University of Medicine and Pharmacy, Bucharest, Romania; [c]Department of Neurology, School of Medicine, Carol Davila University of Medicine and Pharmacy, Bucharest, Romania

ABSTRACT

Regeneration in adult skeletal muscle relies on the activation, proliferation, and fusion of myogenic precursor cells (MPC), mostly resident satellite cells (SC). However, the regulatory mechanism during this process is still under evaluation, with the final aim to manipulate regeneration when the intrinsic mechanism is corrupted. Furthermore, intercellular connections during skeletal muscle regeneration have not been previously thoroughly documented. Our hypothesis was that a direct and close cellular interaction between SC/MPC and invading myeloid cells is a key step to control regeneration. We tested this hypothesis during different steps of skeletal muscle regeneration: (a) the recruitment of activated SC; (b) the differentiation of MPC; (c) myotubes growth, in a mouse model of crush injury. Samples harvested (3 and 5 days) post-injury were screened by light and confocal microscopy. Ultrastructural analysis was performed by conventional transmission electron microscopy (TEM) and scanning transmission electron microscopy (STEM) followed by 3D modeling of electron tomography (ET) data. This revealed a new type of interaction between macrophages and myogenic cells by direct heterocellular surface apposition over large areas and long linear distances. In the analyzed volume, regions spaced below 20 nm, within molecular range, represented 31% of the macrophage membrane surface and more than 27% of the myotube membrane. The constant interaction throughout all stages of myogenesis suggests a potential new type of regulatory mechanism for the myogenic process. Thus, deciphering structural and molecular mechanisms of SC-macrophage interaction following injury might open promising perspectives for improving muscle healing.

ARTICLE HISTORY
Received 24 May 2017
Revised 15 June 2017
Accepted 20 June 2017

KEYWORDS
electron tomography; intercellular contacts; macrophage; myogenic cells; surface apposition; skeletal muscle regeneration; scanning transmission electron microscopy

Introduction

Stem cell therapies with allogenic SC are still of great promise especially for genetic muscle diseases, where autologous transplantation is useless. But this approach too has its shortcomings, like poor cell survival, self-renewal and migration of donor cells, even following local intramuscular injection. This may be due to current culture conditions used for their expansion, which may not be sufficient to maintain the regenerative potential.[1] Consequently, a careful analysis of the cellular and molecular microenvironment during normal regeneration is mandatory for deciphering the interactions leading to efficient cell differentiation.

The incumbent intervention of immune system cells during skeletal muscle regeneration has been extensively studied during the last decade.[2] Following neutrophils, macrophages are the second cell population attracted at the injury site, where they release high amounts of enzymes, cytokines, chemokines and growth factors. Although macrophage subpopulations peak at 3 to 6 days, they are detected in high number even 2 weeks after extensive muscle damage. During the first week post-injury they gradually shift from a pro-inflammatory, phagocytic phenotype (M_1 macrophages) to an anti-inflammatory, non-phagocytic and pro-myogenic phenotype (M_2 macrophages).[3]

More recent studies looking at polarized human macrophage subpopulations proved that the *macrophage phenotypic switch not only follows and assists but, most probably, directs the myogenic time sequence*. Stimulation of proliferation was performed by the pro-inflammatory subtype, when transplanted in tandem with myoblasts.

CONTACT Laura Cristina Ceafalan lauraceafalan@yahoo.com Ultrastructural Pathology Laboratory, Victor Babes National Institute of Pathology, 99–101 Spl. Independentei, 050096, Bucharest, Romania.

Supplemental data for this article can be accessed on the publisher's website.

Moreover, pro-inflammatory macrophages also improved migration and delayed differentiation of the myogenic precursors, as opposed to the anti-inflammatory subpopulation, which facilitated alignment, fusion and further myoblast growth.[4] Similar kinetics of macrophage subtypes and adult myogenesis sequences were demonstrated during normal regeneration in human samples.[5] Though, most studies looking at the involvement of macrophages in the regeneration process have focused on soluble molecules like prostaglandins, cytokines and chemokines,[6] only few reports assumed the importance of intercellular contacts. Sonnet et. al provided evidence for the expression of a set of adhesion molecules that deliver survival signals to myogenic cells.[7] These adhesion molecules were only detected by DNA microarray and then visualized by *in vivo* immunolabelling. However, *in situ* ultrastructural details of direct intercellular contacts have not been investigated so far.

The aim of this study was to assess the existence (in different key moments) of cell-to-cell contacts between activated macrophages and myogenic cells during natural muscle regeneration in a mouse model of acute mechanical injury, to determine the pattern of intercellular interactions and their 3D ultrastructure. Our results showed a constant association between macrophages and myogenic cells at all stages of adult myogenesis, from activated SC, to proliferating and fusing myoblasts up to nascent and growing myotubes, establishing extensive intercellular contacts by tight surface appositions.

Results

The distribution of invading macrophages with respect to myogenic progenitors and nascent myotubes was assessed at selected time-points, 3 and 5 days post-injury, using confocal microscopy for immunolabelled sections (Fig 1 A) and light microscopy for toluidine blue stained semi-thin sections (Fig 1 B).

Both low-magnification approaches showed that in the injured area, the inflammatory infiltrate contains a relatively high proportion of macrophages in each section that was analyzed. These were found most frequently in the vicinity or in close contact with activated SC, myogenic progenitor cells and myotubes during early stages of tissue regeneration. However, this was an uncommon event in non-injured tissue, where macrophages were either very rare or absent in the observed regions.

To further characterize the macrophage-myogenic cells interaction, multiple ultra-thin sections were examined at high-resolution, using TEM (Fig 1 C). These revealed that not only do macrophages accompany myogenic cells in injured muscle, but also establish extensive heterocellular contacts varying from close-range (20–50 nm), to molecular-range appositions (less than 20 nm apart) (Fig 1C and 2). We defined contact regions as tight appositions where the intercellular space measured

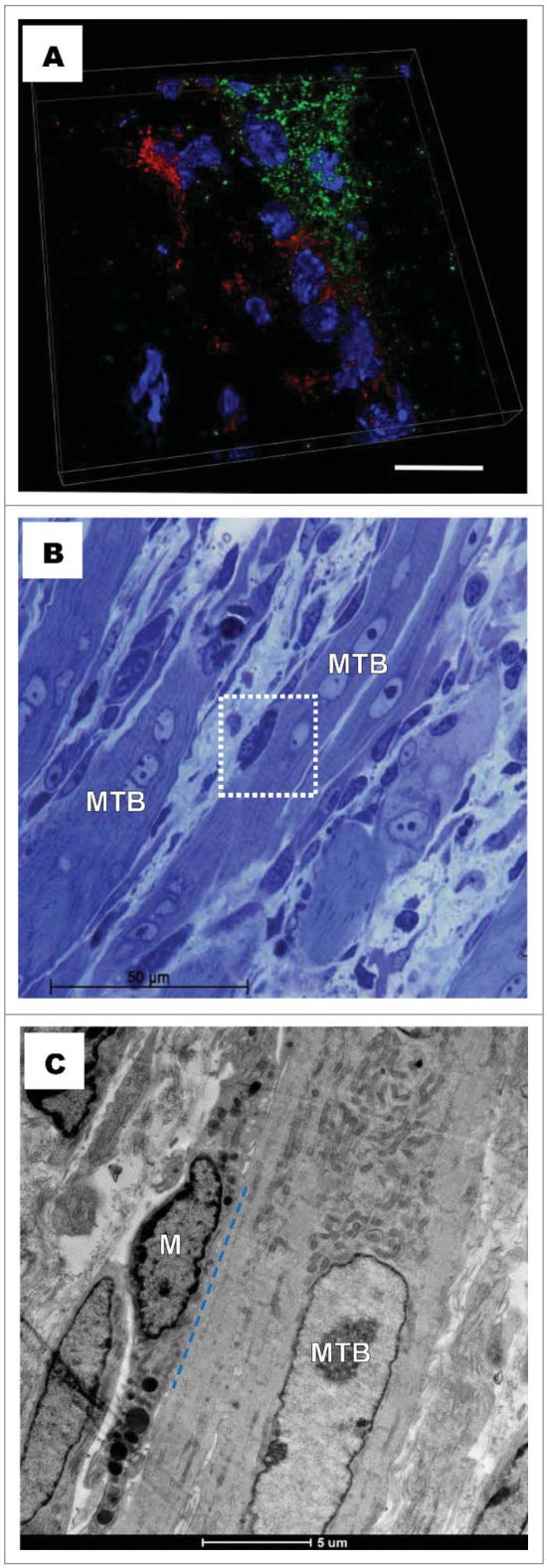

Figure 1. (For figure legend, see page 3.)

below 20 nm, allowing molecular interaction. The average intercellular distance between macrophages and myotubes in regions of tight apposition was 14.2 ± 2.9 nm (n = 50, on 25 different TEM images), extending over variable distances from tens of nm (Fig. 2A, supplemental Fig. 1A) up to tens of μm (Fig. 2C and E). In these regions, the intercellular space was unevenly reduced by electron-dense nanostructures connecting cellular membranes of macrophages and myogenic progenitors (Fig. 2B, Fig. 3).

Widespread macrophage-myoblast interactions were visualized in all stages of myogenesis. As compared to uninjured muscle samples, in the first stages of muscle regeneration post-injury, when SC become activated and then recruited from the niche, they were frequently guarded by macrophages. As compared with quiescent satellite cells,[8] ultrastructural features indicative of SC activation were represented by increased amounts of cytoplasm and organelles (Supplemental Fig. 2). After detaching from the adult muscle fibers, they were regularly found in close contact with activated macrophages (Fig. 2A, supplemental Fig. 2). At this stage, the elongated morphology of macrophages was characteristic of polarized, migrating cells, although the extent and pattern of observed heterocellular contact regions were more suggestive of specific interactions, rather than temporary point contacts (Fig 2B, C, D).

Tight surface appositions were also visualized throughout the next stages of myogenesis, when differentiation occurs and myotubes are formed through myoblast fusion and myofilament organization. In the corresponding ultra-thin sections, planar contacts were found over long linear distances (up to 20 μm, Fig. 1C and Fig. 2E), with electron-dense nanostructures intermittently connecting the cell membranes of the 2 cell types (Fig. 3). Clathrin-coated vesicles (Fig. 2F, Fig. 3A) emerging from the macrophage or myotube membranes were frequently seen and the 2 cell membranes were tightly apposed on both sides of the invagination. Occasionally, weak electron-dense material was observed in the intercellular space where clathrin-coated vesicles emerged (Fig. 2F). Endoplasmic reticulum cisternae and coated or uncoated vesicles were present in the vicinity of planar contacts (Fig. 3) and were also observed in the cortical space of cells involved in the heterocellular contacts. Organization of cytoskeletal elements typical of classical junctions was not observed in the adjacent cortical region of macrophages or myogenic cells. Instead a fuzzy coat of thin filaments could be seen flanking the cellular membranes in contact (Fig. 3).

To better understand the 3D architecture of membrane contacts and to estimate the extent of cell-to-cell interaction, a representative region of heterocellular interaction was selected for STEM electron tomography and volume segmentation (Fig. 4, Supplemental Video 1).

A linear distance of 2650 nm along apposed surfaces was analyzed in 100 consecutive tomogram sections. The average membrane contour lengths were 3147 nm for the myoblast and 2870 nm for the macrophage, respectively. This confirmed that the width of intercellular space varies in regions of apposition throughout the Z direction of the sample volume, suggesting a gradual and specific interaction. The segments where the intercellular space was narrower than 20 nm, appropriate for molecular interactions, were marked in orange in Figure 4. Thus, the marked areas highlighted a patchy distribution of the tight heterocellular apposition. Additionally, electron tomography and 3D modeling allowed the quantification of molecular contacts between cells, revealing that regions spaced below 20 nm represented 31% of the macrophage membrane surface and more than 27% of the myotube membrane in the reconstructed heterocellular contact.

Figure 1. (see previous page.) Mouse gastrocnemius muscle, 5 d post injury. (A). Laser scanning microscopy. Double immunofluorescent labeling shows F4/80 positive macrophages (red) preferentially distributed around growing myotubes (CD56, green). Nuclei were stained with DAPI (blue). Scale bar 20 μm. (B). Light microscopy on toluidine blue-stained semi-thin section of Epon-embedded samples, shows myotubes (MTB) surrounded by inflammatory infiltrate. Square marked area was further examined by transmission electron microscopy (in C). (C). TEM on square marked area in B shows a macrophage (M) which establishes close contacts with a myotube (MTB). The cell membranes of the macrophage and the myotube are closely apposed (15 nm), this apposition extending over 7 μm.

Discussion

Skeletal muscle has a high regeneration potential following various types of injury, with complete structural and functional recovery. This capacity relies on the existence of a local population of myogenic cells that are readily activated by local cues and start their proliferation and subsequent differentiation. The intervention of the initial inflow of inflammatory cells in the regulation of regeneration was long discussed and analyzed[6] up to being declared indispensable.[9] Meddling with the inflammatory response after acute injury proved detrimental to tissue healing.[10] Blocking macrophage infiltration was found to delay SC proliferation and differentiation and to promote fibrosis.[11] Conversely, chronic inflammation accompanying severe myopathies are responsible for secondary damage promoting muscle degeneration and fibrosis.[12,13] Consequently, the intensity, duration and timeline of the inflammatory response as well as

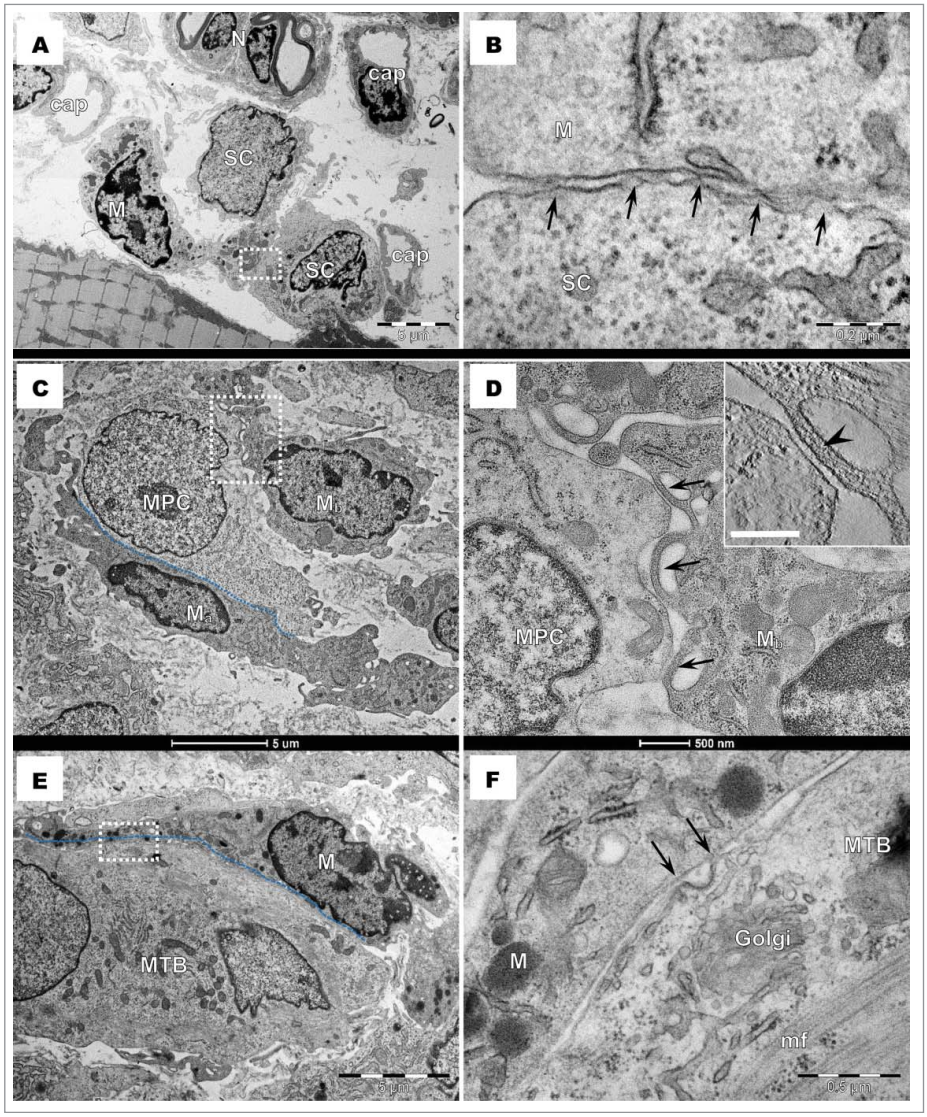

Figure 2. Transmission electron microscopy of gastrocnemius muscle, 5 d after injury. (A). Satellite cell (SC) migrates away from the myofiber and establishes close contacts (rectangular marked area) with a macrophage (M). N – nerve, cap – capillary. (B). Higher magnification of marked area in **A**. shows the apposition of SC and M cell membranes Direct contacts between the 2 cell membranes are visible (arrows). (C). A myogenic precursor cell (MPC) establishes 2 different types of contacts with macrophages (M): a planar contact (dotted line) extending over 10 μm and point contacts (rectangular marked area, enlarged in **D**). (D). Convex pseudopodial extensions (arrows) of the macrophage (Mb), containing thin filaments (arrowhead in the inset), fit MPC cytoplasmic protrusions. (E). A planar contact (blue dotted line) is visible between a macrophage (M) and a myotube (MTB), and extends over 15 μm. (F). Higher magnification of rectangular marked area in **E**. reveals details of the planar contact between M and MTB. Arrows indicate point contacts on both sides of a coated pit which contains a weak electron-dense material. Golgi and myofilaments (mf) are visible in the cytoplasm of the MTB.

myeloid cell phenotype switches must strictly coordinate with tissue regeneration time-points for efficient repair.

However, most of the work focused on paracrine signals released by the invading activated myeloid population, mostly macrophages, that modulate the transcriptional activity of myogenic cells,[14] while the ultrastructural evidence to support this interaction was lacking. In this study we used high resolution imaging techniques to characterize for the first time the interaction between macrophages and myoblasts at different stages of myogenesis, in injured skeletal muscle.

Our results revealed that macrophages and myogenic cells establish cell-to-cell contacts following sterile crush injury in normal mice, all throughout the myogenic process starting with the recruitment of activated SC and following the differentiating myogenic cells up to growing myotubes.

We documented the existence of direct, close contacts between myogenic cells and macrophages, such as: a) tight surface apposition, over large areas and long linear distances, infrequently interrupted by coated pits and caveolae; b) point contacts by

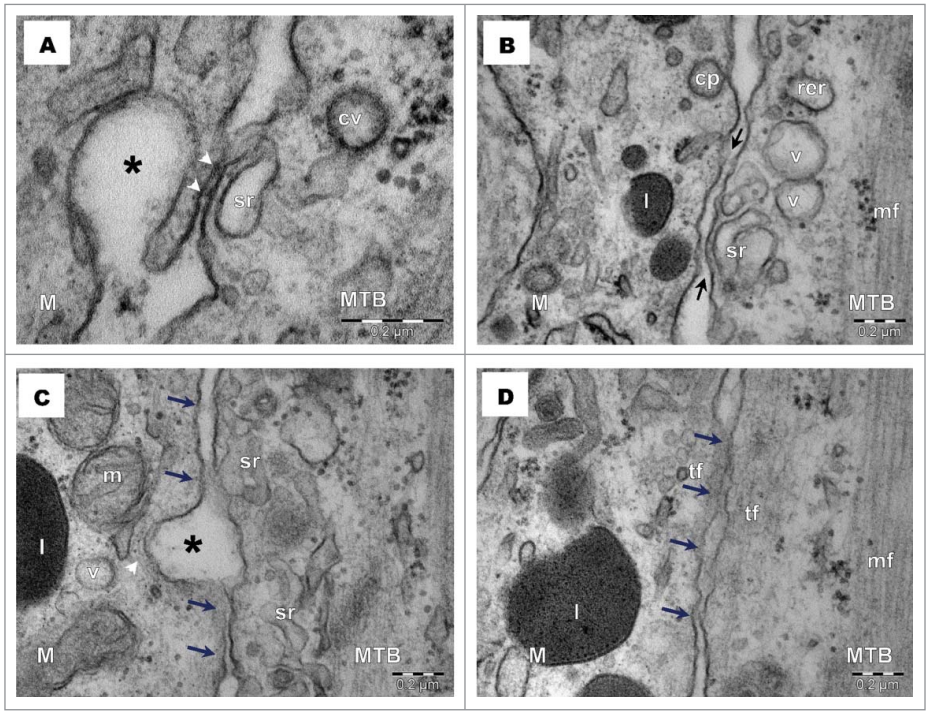

Figure 3. Transmission electron microscopy of gastrocnemius muscle, 5 d after injury. (A). Electron-dense nanostructures (arrowheads) fasten the contact between a macrophage (M) and a myotube (MTB). The sarcoplasmic reticulum (sr) of the myotube is also connected with the sarcolemma by dense nanostructures. A coated vesicle (cv) is visible in the cortical space of the myotube, in the vicinity of contact. (B). The close membrane apposition of a macrophage (M) and a myotube (MTB) is mediated by electron-dense material (between arrows). Uncoated vesicles (v), sarcoplasmic reticulum (sr) and a coated pit (cp) are visible near the plasma membranes of the cells in contact. l – lysosome; rer – rough endoplasmic reticulum. (C). Electron-dense material connects (arrows) the membranes of a macrophage (M) and a myotube (MTB) on both sides of the macrophage membrane invagination (*). Cortical cytoskeleton filaments (arrowhead) bend around this invagination. (D). Thin filaments (tf) form a fuzzy coat beneath both macrophage (M) and myotube (MTB) cell membrane. Electron-dense nanostructures are present in the intercellular space (arrows). mf – myofilaments.

macrophage pseudopodial extensions and myogenic cell cytoplasmic protrusions.

Besides a potentially direct effect through cell-to-cell adhesion, a tight surface apposition that narrows the intercellular space down to tens of nanometers could facilitate intercellular communication through soluble molecules. A very large array of small molecules can modulate the epigenetic environment to maintain a balance between myogenesis and fibrogenesis. Moreover, this extensive patchwork of molecular-range appositions likely favors other types of intercellular communication, such as the recently described transfer of non-coding RNAs, implicated in the epigenetic modulation of cell behavior.[15]

Indeed, we frequently found these contacts in the vicinity of specialized structures, such as caveolae, coated pits, invaginations and sarcoplasmic reticulum, strongly suggesting specific secretory activity. This hypothesis was further reinforced by the presence of electron-dense particles at tight contacts sites, which appeared to bridge intercellular gaps.

Therefore, alongside other local cues, the invading myeloid cell population seems to establish a microenvironment where not only the vast array of soluble molecules, but also direct molecular contacts organize specific timeframes for *in vivo* muscle regeneration.

Interestingly, the complex patchwork of tight contacts was maintained in the Z-axis, as revealed by STEM tomography. This technique, augmented by segmentation and 3D modeling, is becoming indispensable to obtaining high resolution data of thick biological specimens[16] (Supplemental Video 1).

The ultrastructural features of this heterocellular interaction were exceedingly similar to the apposition and flattening observed between myoblasts and myotubes before cell fusion[17] (Supplemental Fig. 1).

Together, these data suggest a specific and gradual type of interaction between macrophages and myoblasts in injured muscle tissue, different from the classical temporary point contacts, focal complexes and podosomes used for traction during macrophage migration,[18] as motility is a key feature of their generally accepted, yet continuously expending, set of functions.

The results of this study disclose a new dimension on cellular cooperation, supporting the emerging hypothesis that co-transplantation represents one direction to potentially optimize the outcome of cell-based therapies.

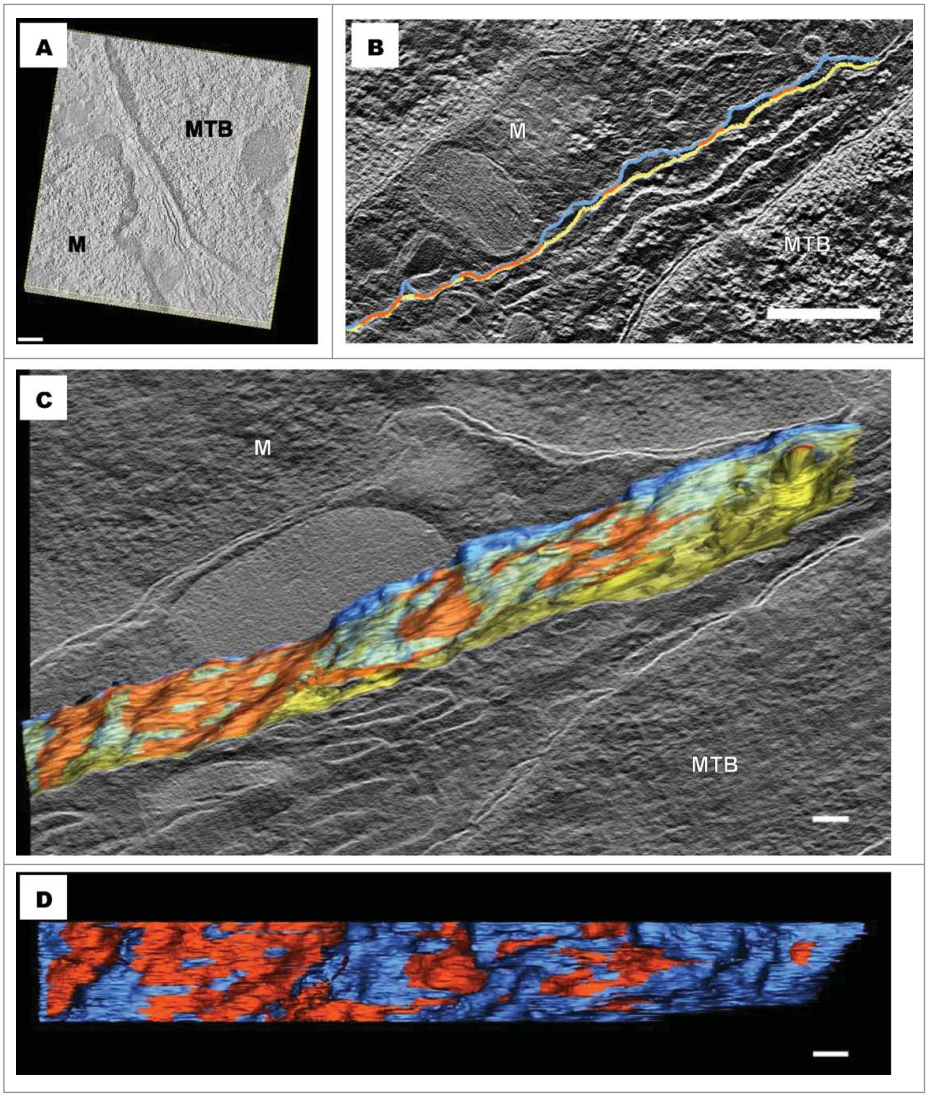

Figure 4. STEM tomography of intercellular contacts. (A) Reconstructed tomogram of a contact region between a macrophage (M) and a myoblast (MTB); (B) Tomogram section with superimposed drawn contours, highlighting the relatively spread out contact area. The macrophage membrane is shown in blue, the myoblast membrane in yellow and tight appositions in orange; (C) Overlay of one tomographic section and the 3D render of the macrophage-myoblast membranes, obtained from the segmentation data. Transparency was adjusted for the myoblast membrane (yellow), to allow viewing of contact regions; (D) 3D model, showing the macrophage membrane external surface and associated contact sites. These account for more than 30% of the total membrane surface. Scale bars represent 500 nm for images A and B, and 200 nm for images C and D.

Moreover, the close cooperation between macrophages and myoblasts could open a new perspective for the development of effective targeted therapies for genetic defects.

Materials and methods

Animal model

Experiments were performed in accordance with international guidelines and were approved by the ethics committee of Victor Babes Institute of Pathology. To minimize unnecessary suffering, the mice were anesthetized by the intramuscular injection of 100 mg/kg Ketamine (Kepro B.V.) in the anterior left leg before the procedure and before being killed by cervical dislocation. The animal model that simulates clinical condition of muscle contusion injury consisted in crushing the left leg of 10 week-old *C57BL/6J* (The Jackson Laboratory # 000664) mice with an adjusted forceps, 1 cm away from the distal joint. The pressure was maintained for 2 min. Crushed gastrocnemius muscle was dissected and collected at different time-points starting 24 h post-injury and then during the 3rd and 5th day. These time-points correspond to the peak concentrations of infiltrating macrophage in the injured area, 72–96 h post injury for pro-inflammatory M1 sub-

population and around 120 h post-injury for M2, anti-inflammatory sub-population.[3]

Immunofluorescence

For immunolabelling experiments the samples were quickly frozen in liquid nitrogen and stored in deep-freezing compartments. Sections (4 μm thick) were fixed in acetone at −20°C for 5 min and then rehydrated in PBS for 10 min. Incubation overnight at 4°C, with rat anti-mouse F4/80 (1:50, ab16911 Abcam), was followed by 1 h incubation with goat anti-rat AlexaFluor 647 conjugated secondary antibody (1:300, A21247 Molecular Probes), at room temperature. To saturate open binding sites on this first secondary antibody, the sections were further incubated for 1 h with 2% normal rat serum. Slides were then treated with excess unconjugated goat anti-rat Fab fragment (10 μg/ml, #112–007–003 Jackson ImmunoResearch) for covering open binding sites on rat IgG to prevent non-specific binding of the other secondary antibody. This step was followed by light fixation with 4% formaldehyde. Incubation with the second primary antibody, rat anti-mouse CD56 (1:100, ABIN809963 Antibodies Online) was performed overnight at 4°C, followed by 1 h incubation with AlexaFluor 488 conjugated donkey anti-rat secondary antibody (1:300, A21208, Molecular Probes). Nuclei were stained with 4′,6-diamidino-2-phenylindole (DAPI) (Sigma-Aldrich). Negative controls were obtained by the same protocol, but omitting the primary antibody and with isotype control. Sections were mounted with Fluorescence Mounting Medium (Dako) and analyzed on a Leica TCS SP8 Confocal laser scanning system (Leica Microsystems, Germany), using an oil immersion HC PL APO CS2 100 x/1.40NA objective. A 405 nm UV laser was used for imaging DAPI, whereas for AlexaFluor 488 and 647 optimal excitation wavelengths were selected using a white light laser source (tunable range between 470 and 670 nm, at 1 nm intervals). Emission was registered using PMT or HyD detectors, respectively. Image acquisition was done using the manufacturer supplied LASX software (Leica Microsystems) and deconvolution with Huygens package (Scientific Volume Imaging).

Transmission electron microscopy (TEM)

Small fragments of gastrocnemius muscle from perilesional and lesional areas were fixed by immersion in 4% glutaraldehyde, post-fixed in buffered 1% OsO_4 1.5% $K_4Fe(CN)_6$ (potassium ferrocyanide-reduced osmium), dehydrated in graded ethanol series and further processed for epoxy resin embedding (AGAR 100). - 1 μm-thick sections (semi-thin sections) were stained with 1% toluidine blue and examined by light microscopy before ultra-thin sectioning. Ultra-thin sections were cut with a diamond knife at 60 nm thickness using a Leica EM UC7 ultramicrotome (LM) and double stained with uranyl acetate and lead citrate. Ultrastructural analysis was performed using a Morgagni 286 TEM (FEI Company) running at 80 kV. Digital electron micrographs were recorded with a MegaView III CCD and iTEM-SIS software (Olympus) was used for morphometry.

Electron tomography and 3D modeling

STEM tomography was performed on 300 nm thick sections using the HAADF detector of a 200 kV Talos F200C S/TEM (FEI Company). The single axis tilt series was collected using FEI STEM tomography software, at 10 s dwell time and a nominal magnification of 18000x, with giving a final object sampling of 2.47 nm/pixel. The angular tilt range was between −60° and +60°, with increments of 2°. Tilt series images were aligned and reconstructed using the IMOD-eTOMO package.[19] One representative tomogram was chosen for segmentation in IMOD, on which membranes and adjacent structures were manually traced on 100 virtual slices to obtain a 3D model. All measurements were generated using *imodinfo*. Short animations were compiled using the freely available video-editing software VideoMach (http://gromada.com/videomach/).

Disclosure of potential conflicts of interest

No potential conflicts of interest were disclosed.

This work was supported by the Romanian National Authority for Scientific Research (CNCS-UEFISCDI) under Grant PN-II-RU-TE-2011–3–0206 (grant no. 32/2011); Minister of Research and Innovation under grant number PN16.22/31N/2016.

References

[1] Kuang S, Rudnicki MA. The emerging biology of satellite cells and their therapeutic potential. Trends Mol Med 2008; 14:82-91; PMID:18218339; https://doi.org/10.1016/j.molmed.2007.12.004

[2] Tidball JG. Inflammatory processes in muscle injury and repair. Am J Physiol Regul Integr Comp Physiol 2005; 288:R345-53; PMID:15637171; https://doi.org/10.1152/ajpregu.00454.2004

[3] Saini J, Mcphee JS, Al-Dabbagh S, Stewart CE, Al-Shanti N. Regenerative function of immune system: Modulation of muscle stem cells. Ageing Res Rev 2016; 27:67-76; PMID:27039885; https://doi.org/10.1016/j.arr.2016.03.006

[4] Bencze M, Negroni E, Vallese D, Yacoubâ€“Youssef H, Chaouch S, Wolff A, Aamiri A, Di Santo JP, Chazaud B, Butler-Browne G, et al. Proinflammatory Macrophages Enhance the Regenerative Capacity of Human Myoblasts

by Modifying Their Kinetics of Proliferation and Differentiation. Mol Ther 2012; 20:2168-79; PMID:23070116; https://doi.org/10.1038/mt.2012.189

[5] Saclier M, Yacoub-Youssef H, Mackey AL, Arnold L, Ardjoune H, Magnan M, Sailhan F, Chelly J, Pavlath GK, Mounier R, et al. Differentially activated macrophages orchestrate myogenic precursor cell fate during human skeletal muscle regeneration. Stem Cells 2013; 31:384-96; PMID:23169615; https://doi.org/10.1002/stem.1288

[6] Tidball JG, Villalta SA. Regulatory interactions between muscle and the immune system during muscle regeneration. Am J Physiol Regul Integr Comp Physiol 2010; 298:R1173-87; PMID:20219869; https://doi.org/10.1152/ajpregu.00735.2009

[7] Sonnet C, Lafuste P, Arnold L, Brigitte M, Poron F, Authier FJ, Chrétien F, Gherardi RK, Chazaud B. Human macrophages rescue myoblasts and myotubes from apoptosis through a set of adhesion molecular systems. J Cell Sci 2006; 119:2497-507; PMID:16720640; https://doi.org/10.1242/jcs.02988

[8] Günther S, Kim J, Kostin S, Lepper C, Fan CM, Braun T. Myf5-positive satellite cells contribute to Pax7-dependent long-term maintenance of adult muscle stem cells. Cell Stem Cell 2013; 13(5):590-601; PMID:23933088; https://doi.org/10.1016/j.stem.2013.07.016

[9] Merly F, Lescaudron L, Rouaud T, Crossin F, Gardahaut MF. Macrophages enhance muscle satellite cell proliferation and delay their differentiation. Muscle and Nerve 1999; 22:724-32; PMID:10366226; https://doi.org/10.1002/(SICI)1097-4598(199906)22:6%3c724::AID-MUS9%3e3.0.CO;2-O

[10] Shen W, Li Y, Tang Y, Cummins J, Huard J. NS-398, a cyclooxygenase-2-specific inhibitor, delays skeletal muscle healing by decreasing regeneration and promoting fibrosis. Am J Pathol 2005; 167:1105-17; PMID:16192645

[11] Segawa M, Fukada S, Yamamoto Y, Yahagi H, Kanematsu M, Sato M, Ito T, Uezumi A, Hayashi S, Miyagoe-Suzuki Y, et al. Suppression of macrophage functions impairs skeletal muscle regeneration with severe fibrosis. Exp Cell Res 2008; 314:3232-44; PMID:18775697

[12] Villalta SA, Nguyen HX, Deng B, Gotoh T, Tidball JG. Shifts in macrophage phenotypes and macrophage competition for arginine metabolism affect the severity of muscle pathology in muscular dystrophy. Hum Mol Genet 2009; 18:482-96; PMID:18996917

[13] Bosurgi L, Manfredi AA, Rovere-Querini P. Macrophages in injured skeletal muscle: A perpetuum mobile causing and limiting fibrosis, prompting or restricting resolution and regeneration. Front Immunol 2011; 2:1-10; PMID:22566792

[14] Ceafalan LC, Popescu BO, Hinescu ME. Cellular players in skeletal muscle regeneration. Biomed Res Int 2014; 2014:957014; PMID:24779022

[15] Yang M, Chen J, Su F, Yu B, Su F, Lin L, Liu Y, Huang J-D, Song E. Microvesicles secreted by macrophages shuttle invasion-potentiating microRNAs into breast cancer cells. Mol Cancer 2011; 10:117; PMID:21939504

[16] Yakushevska AE, Lebbink MN, Geerts WJC, Spek L, van Donselaar EG, Jansen KA, Humbel BM, Post JA, Verkleij AJ, Koster AJ. STEM tomography in cell biology. J Struct Biol 2007; 159:381-91; PMID:17600727

[17] Dhanyasi N, Segal D, Shimoni E, Shinder V, Shilo BZ, VijayRaghavan K, Schejter ED. Surface apposition and multiple cell contacts promote myoblast fusion in Drosophila flight muscles. J Cell Biol 2015; 211:191-203; PMID:26459604

[18] Pixley FJ. Macrophage migration and its regulation by CSF-1. Int J Cell Biol 2012; 2012:501962; PMID:22505929

[19] Kremer JR, Mastronarde DN, McIntosh JR. Computer visualization of three-dimensional image data using IMOD. J Struct Biol 1996; 116:71-6.